

1H MRS and MRI longitudinal study to detect therapeutic response in non-Hodgkin's lymphoma patients

S-C. Lee¹, H. Poptani¹, H. Hariharan¹, S. Nasta², J. Svoboda², S. J. Schuster², and J. D. Glickson¹

¹Department of Radiology, University of Pennsylvania, Philadelphia, PA, United States, ²Department of Medicine, Hematology Oncology Division, University of Pennsylvania, Philadelphia, PA, United States

INTRODUCTION Non-Hodgkin's lymphoma is the fifth most common cancer in the United States. During the last 50 years, its incidence has increased two-fold. The primary method of diagnostic imaging of this disease is by PET-CT, which detects the influx and retention of ¹⁸F-2-deoxyglucose by cancer cells, which is diminished after successful therapy. As PET requires administration of a radioactive tracer and fasting before imaging, we explored the use of more convenient and potentially less hazardous MRS and MRI methods for early detection of therapeutic response. In preclinical lymphoma studies in animal models, we demonstrated that ¹H MRS and MRI provide sensitive markers for chemotherapy, immunotherapy and radiation therapy. Lactate and the apparent diffusion coefficient (ADC) are sensitive indices of response to chemotherapy and radiation therapy, while total choline is an indicator of response to immunotherapy and radiation therapy [1-3]. We have recently developed a Hadamard slice-encoded selective multiple quantum coherence sequence for lactate detection and implemented it on a clinical scanner [4]. The lactate imaging method and the single voxel PRESS and multi-slice diffusion-weighted imaging (DWI) sequences were utilized in this preliminary study of non-Hodgkin's lymphoma patients.

METHODS The multi-slice lactate imaging sequence was previously demonstrated to produce high quality localized images of lactate in an NHL patient [4]. The sequence starts with a Hadamard encoded adiabatic slice inversion pulse for multi-slice selection. A selective multiple quantum coherence (Sel-MQC) pulse train follows thereafter; 90° (CH₃) -1/2J- 90° (CH) - 180° (CH₃) - 90° (CH₃)-1/2J-ACQ. Coherence selection gradients were inserted in the Sel-MQC pulse train between the second and third RF pulses and after the fourth RF pulse to select the double quantum to zero quantum transition of J-coupled lactate (CH₃) spins (1.3 ppm) while spoiling the signal of uncoupled lipid resonances resonating at the same frequency. 2D-CSI encoding gradients were placed after the last RF pulse. A Hadamard-slice encoded water spin echo CSI sequence was run for calibration. Total choline was measured using a single voxel PRESS sequence with outer volume suppression; TR=1500 ms, TE=135 ms. Unsuppressed water signals in the same voxel were used for calibration. The ADC was measured using a diffusion-weighted echo planner imaging (DW-EPI) sequence. B-values of 0, 250 s/mm², 500 s/mm², and 750 s/mm² were used. All measurements were performed on a 3T Siemens Trio system with the VB17 IDEA software. The Had-Sel-MQC-CSI raw data were retrieved using the TWIX command in the scanner and processed with an in-house IDL program. The PRESS spectral data were exported in .rda format and processed using NUTs software (Acorn NMR). ADC maps were generated using a Siemens-provided processing routine. MRS/MRI measurements were performed before treatment and within one week after initiation of treatment.

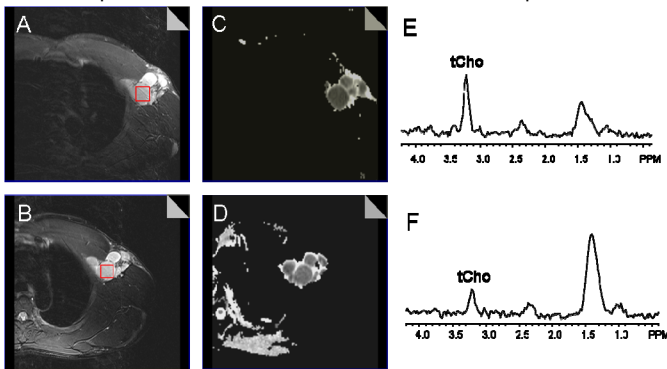


Fig 1. Longitudinal MR measurements of a 44 yo male follicular lymphoma patients before and after treatment (upper panels and lower panels respectively). Left: T2-weighted images, middle: ADC maps, right: PRESS spectra.

RESULTS Fig 1 shows data from a lymphoma patient with a lesion in the axillary node. Fig 1A, 1C and 1E are the T2-weighted image, ADC map and PRESS spectrum of the patient before treatment. Fig 1B, 1D and 1F are corresponding images and spectrum 4 days after initiation of therapy. An

increase of ADC and decrease of tCho were observed. Quantitative changes appear in the Penn-3 row of Table 1. Table 1 summarizes the results of three non-Hodgkin's lymphoma patients who participated in this preliminary longitudinal MRS/MRI study. The patient Penn-1 exhibited complete

Patient ID	NHL type, region	Age, gender	Therapeutics	MRI/MRS timing to treatment initiation	Tumor volume change	Lac/H2O change	tCho/H2O change	ADC change
Penn-1	DLBCL, inguinal, naive	63, M	RCHOP	2 days prior, 2 days after	25% ↓	70% ↓	15% ↑	Not measured.
Penn-2	DLBCL, neck, naive	46, M	RCHOP	15 days prior, 4 days after	34% ↓	Not measured.	4% ↓	9% ↑
Penn-3	follicular, axillary, recurrent	44, M	Rituxan + Bendamustine	2 days prior, 4 days after	15% ↓	30% ↓	50% ↓	36% ↑

Table 1. Summary of longitudinal studies of three non-Hodgkin's lymphoma patients.

remission as observed at 6 month and continues at 2 years from treatment. Patient Penn-3 is in remission as of 5 month after treatment. The status of the patient Penn-2 is still being evaluated. The trend shows a decrease of Lac and tCho and increase of ADC after treatment. In one patient tCho increased rather than decreased. In view of our xenograft study [2], this may indicate that the patient is refractory to rituximab treatment, but further studies are required to confirm this conclusion.

DISCUSSION These initial studies of three NHL patients clearly

demonstrate that MRS/MRI methods can detect early treatment responses within about 48 hr in non-Hodgkin's lymphoma patients.

REFERENCES

[1] Lee et al., In vivo MRS markers of response to CHOP chemotherapy in the WSU-DLCL2 human diffuse large B-cell lymphoma xenograft. NMR Biomed 21:723-733, 2008. [2] Lee et al., In vivo ¹H MRS of WSU-DLCL2 human non-Hodgkin's lymphoma xenografts: response to rituximab and rituximab plus CHOP. NMR Biomed 22:259-265, 2009. [3] Lee et al., Early detection of radiation therapy response in non-Hodgkin's lymphoma xenografts by in vivo ¹H magnetic resonance spectroscopy and imaging. NMR Biomed 23:624-632, 2010. [4] Mellon et al., Detection of lactate with a hadamard slice selected, selective multiple quantum coherence, chemical shift imaging sequence (HDMD-SelMQC-CSI) on a clinical MRI scanner: Application to tumors and muscle ischemia. Magn Reson Med 62:1404-1413, 2009.

ACKNOWLEDGEMENT. NIH 2R01-CA101700, R01-CA118559.